Variations in crystals of flufenamic acid of its methyl and *tert*-butyl analogues as impurities as determined by partial dissolutions

Timothy Bourke[a], Renato A. Chiarella[b] and Humphrey A. Moynihan[a*]

[a]Analytical and Biological Chemistry Research Facility / Synthesis and Solid State Pharmaceutical Centre / School of Chemistry, University College Cork, College Road, Cork Y12 K8AF, Ireland.

[b]Pharmaceutical Development, Alkermes Inc., 900 Winter Street, Waltham, MA 02451, USA.

Supplementary Information

Synthetic methods

*Preparation of 2-(3-tolylamino)benzoic acid (MeFA) and 2-((3-(*tert*-butyl)phenyl)amino)benzoic acid (t*BuFA)*

2-Chlorobenzoic acid (1.25 g, 8 mmol) was added to a 100 mL round bottomed flask with potassium carbonate (0.55 g, 4 mmol) and metallic copper (40 mg, 0.63 mmol). The flask was flushed with N_2 gas. The desired substituted aniline (16 mmol) and anhydrous *N*,*N*-dimethylformamide (5 mL) were added through a septum. The reaction was refluxed at 155 °C for 4 hours. The reaction mixture was cooled, then slowly added to 1:1 aqueous hydrochloric acid (20 mL with washings) and allowed to stand overnight. The precipitate was isolated *via* vacuum filtration and rinsed with dilute hydrochloric acid. The solid was redissolved in ethyl acetate, activated charcoal (*ca*. 1 g) added, and the mixture filtered through Celite®. The filtrate was extracted with boiling water (3 x 30 mL) and dried over anhydrous magnesium sulfate. The solvent was removed by rotary evaporation to isolate the crude product which was purified by wet flash chromatography using silica gel 60 Å, 200 - 425 mesh particle size (Sigma Aldrich) and an eluent of, initially, 5% v/v MeOH in dichloromethane increasing gradually to a maximum of 10% v/v.

Characterisation Information

NMR Spectroscopy, IR spectroscopy and mass spectrometry

^{1}H NMR spectra were recorded at 300 MHz on a Bruker AVANCE 300 NMR spectrometer or at 400 MHz on a Bruker AVANCE 400 NMR spectrometer. ^{13}C NMR spectra were recorded at 100.6 MHz on a Bruker AVANCE 400 NMR spectrometer. IR spectra were recorded on a Perkin Elmer Spectrum 100 FT-IR Spectrometer. High resolution mass spectra (HRMS) were recorded

on a Waters LCT Premier Time of Flight spectrometer (KD160) or a Waters Vion IMS Mass Spectrometer (SAA0 55K) in ESI mode using 50% acetonitrile / water containing 0.1% formic acid as an eluent. Mass spectrometry samples were prepared in acetonitrile.

2-(3-Tolylamino)benzoic acid (MeFA)

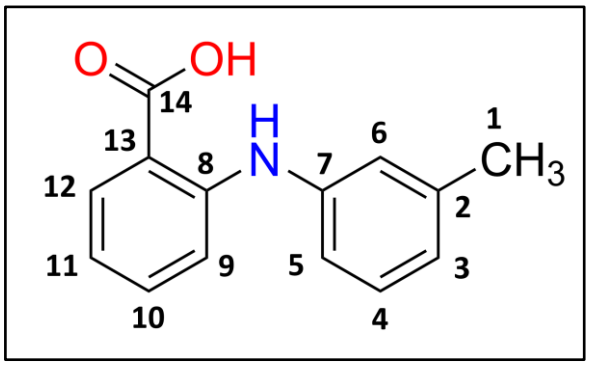

Yellow, needle-like crystals; m.p. 136.6-139.3 °C (Lit.[S1] 136-137 °C); IR ν_{max} (cm^{-1}) (NaCl) 3341 (amine N-H stretch), 3038, 2639 (alkyl C-H stretches), 2921 (acid O-H stretch), 1661 (acid C=O stretch), 1577 (ar. C-C stretch), 1515 (amine N-H bend), 1452 (acid O-H bend), 1243, 1162 (C-N stretches), 901, 779, 747, 694, 649 (ar. C-H bends); ^{1}H NMR 300 MHz, δ_H (MeOD) 2.34 (3H, s, C(1)*H*$_3$), 6.71-6.76 (1H, t, *J* 7.8 Hz, C(11)*H*), 6.87-6.90 (1H, d, *J* 7.8 Hz, C(5)*H*), 7.00-7.02 (2H, m, C(3)*H* and C(6)*H*), 7.20-7.25 (2H, m, C(9)*H* and C(10)*H*), 7.36-7.42 (1H, ddd, *J* 7.8, 7.8 1.2 Hz, C(4)*H*), 7.97-8.00 (1H, dd, *J* 7.8, 1.2 Hz, C(12)*H*), O*H* and N*H* signals not observed; ^{13}C NMR 100.6 MHz, δ_C (MeOD) 21.51 (*C*(1)H$_3$), 113.40 (*C*(13)), 114.97 (*C*(9)H), 118.03 (*C*(5)H), 120.15 (*C*(11)H), 123.80 (*C*(6)H), 125.25 (*C*(3)H), 130.25 (*C*(4)H), 133.28 (*C*(12)H), 135.10 (*C*(10)H), 140.47 (*C*(2)), 142.17 (*C*(7)), 149.44 (*C*(8)), 171.88 (*C*(14)); HPLC retention time 1.70 min, 0.78 relative to FFA; m/z (ESI+): 228.3 $[M+H]^+$, HRMS: $C_{14}H_{13}NO_2$, Predicted m/z 228.101905, Measured m/z 228.10167 $[M+H]^+$, i-FIT Confidence (%) 100.000000.

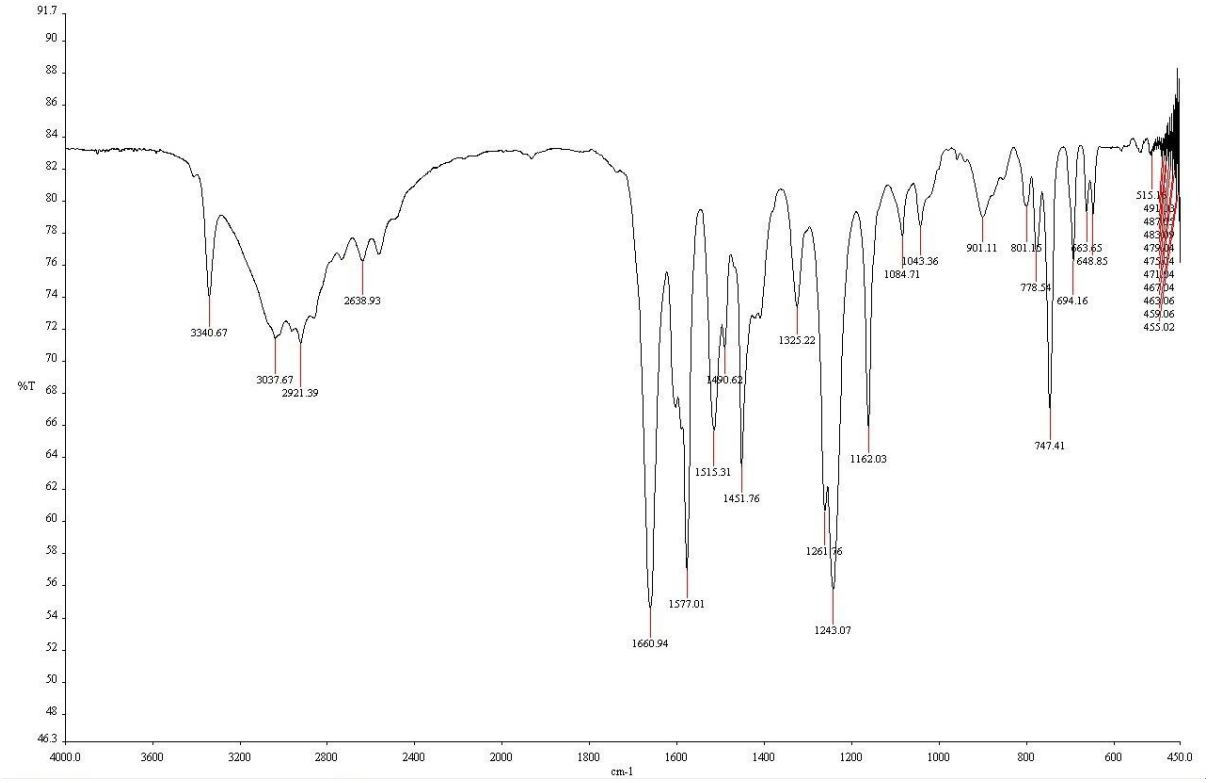

FigS1. IR spectrum of MeFA.

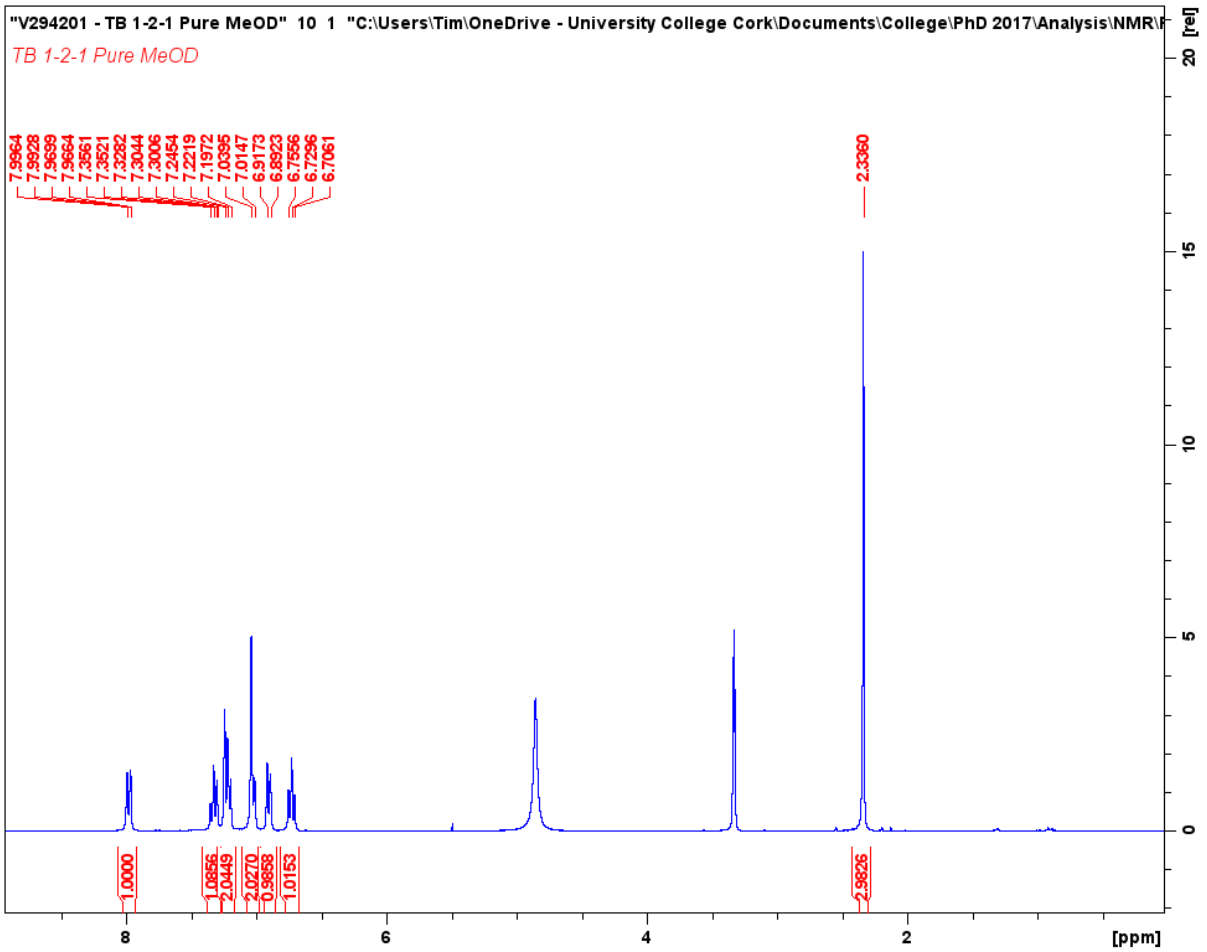

Fig S2. Full ^{1}H NMR spectrum of MeFA

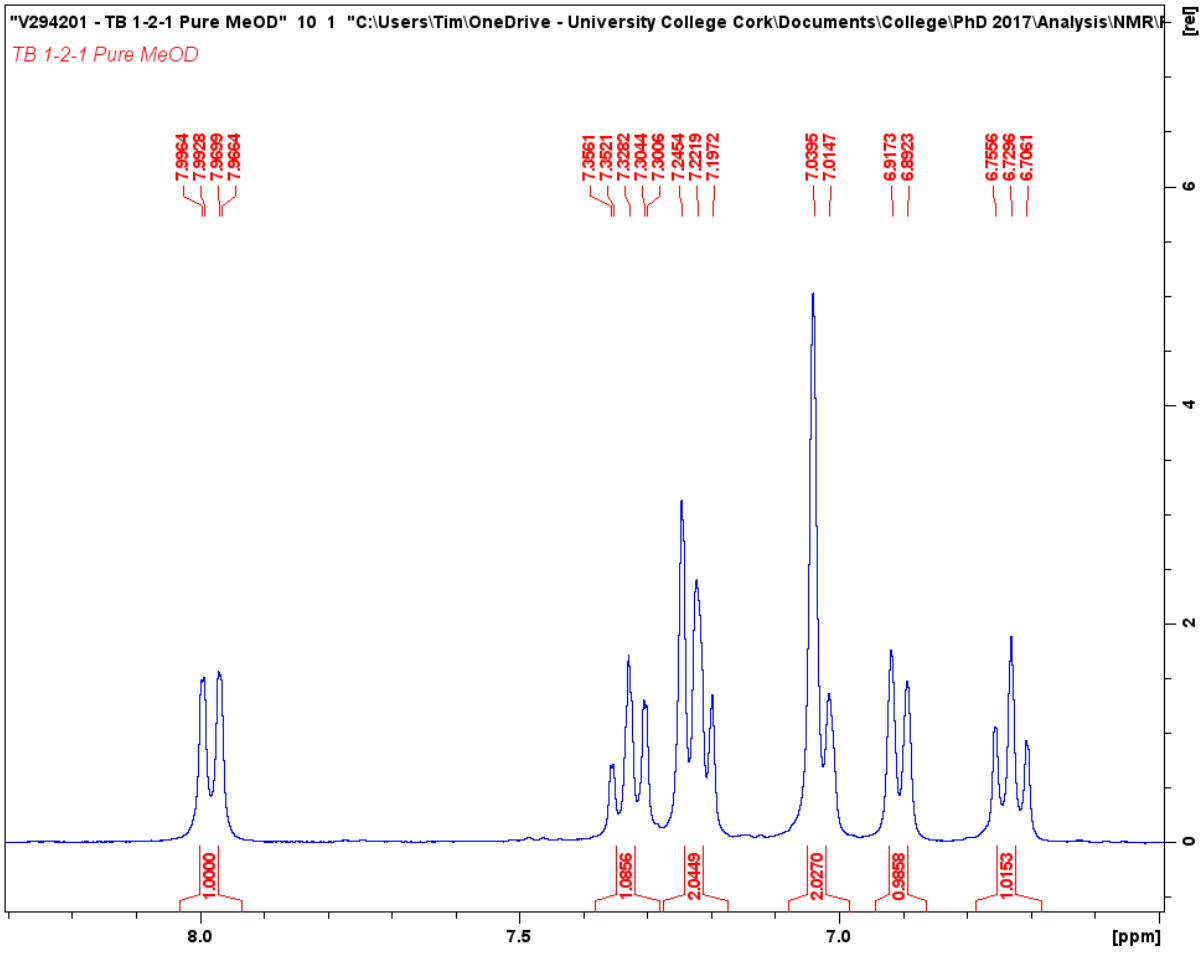

Fig S3. Aromatic region of the ^{1}H NMR spectrum of MeFA.

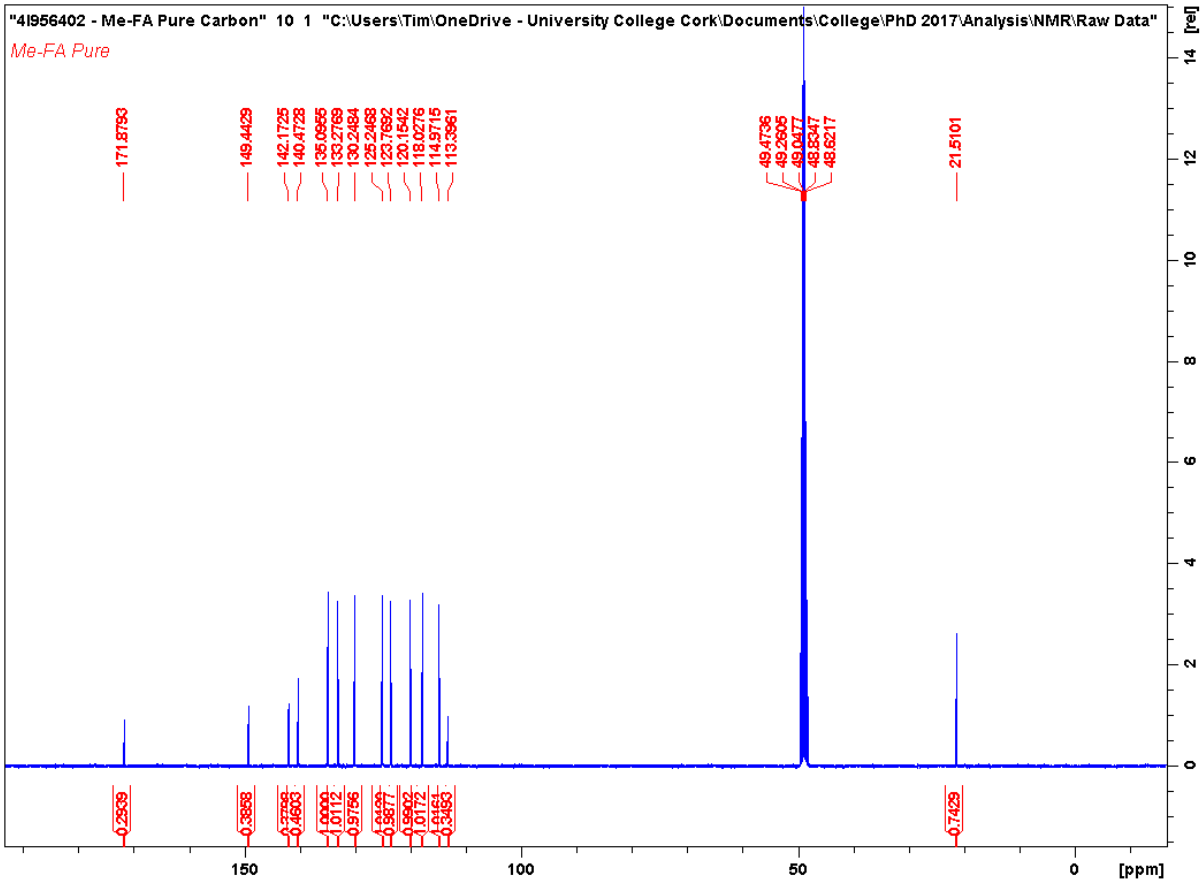

Fig S4. Full ^{13}C NMR spectrum of MeFA, showing the position of the C^1 methyl signal outside the aromatic region.

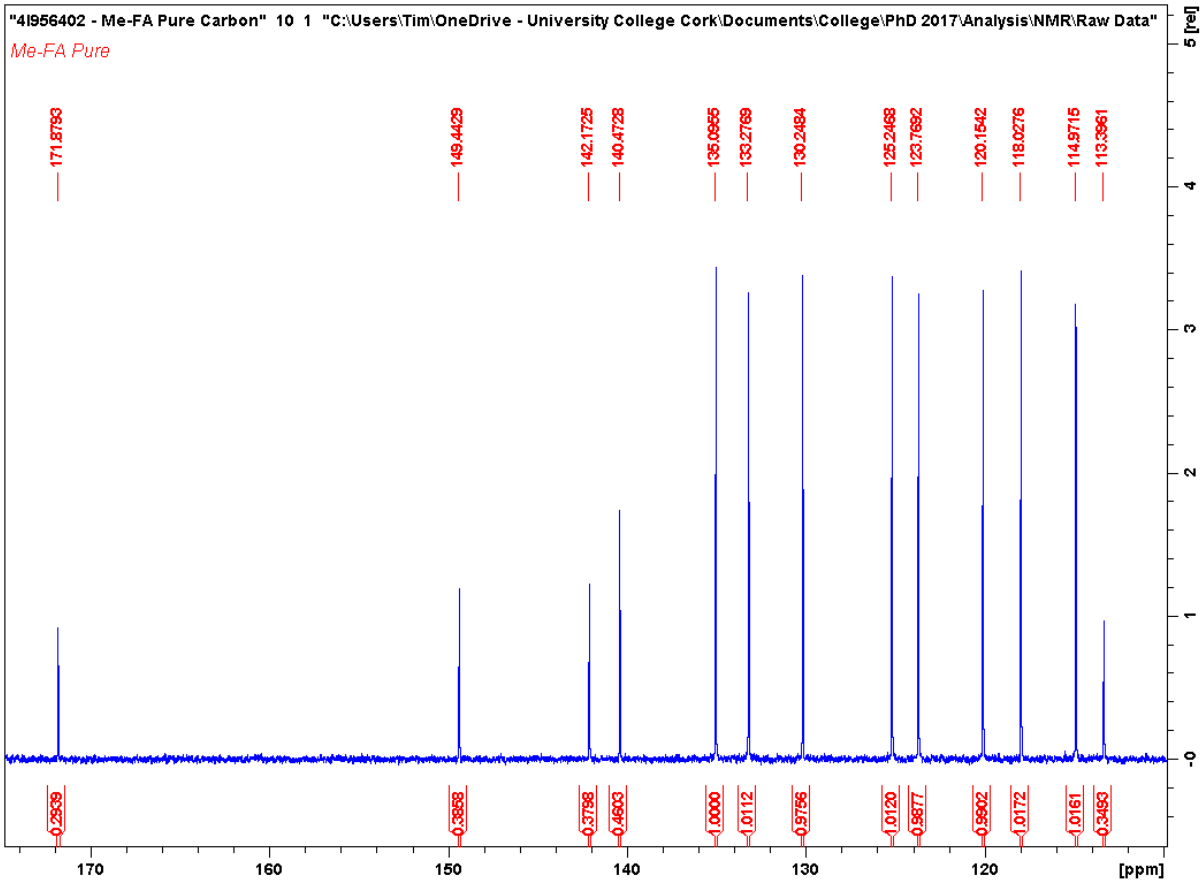

Fig S5. Aromatic region of the ^{13}C NMR spectrum of MeFA.

*2-((3-(*tert*-Butyl)phenyl)amino)benzoic acid (tBuFA)*

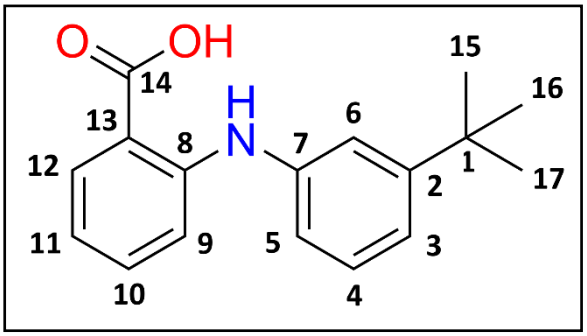

Pale yellow powder; m.p. 153.1-154.0 °C (lit.[S2] 151-153 °C); IR ν_{max} (cm^{-1}) (NaCl) 3349 (amine N-H stretch), 2963 (acid O-H stretch), 2869, 2638, 2563 (alkyl C-H stretches), 1661 (acid C=O stretch), 1575 (ar. C-C stretch), 1514 (amine N-H bend), 1452 (acid O-H bend), 1246, 1162 (C-N stretches), 891, 782, 748, 700, 653 (ar. C-H bends); ^{1}H NMR 400 MHz, δ_H (MeOD) 1.30 (9H, s, C(15)*H*$_3$ and C(16)*H*$_3$ and C(17)*H*$_3$), 6.68-6.72 (1H, ddd, *J* 7.5, 7.5, 1.4 Hz, C(11)*H*), 7.02-7.04 (1H, d, *J* 7.8 Hz, C(5)*H*), 7.10-7.12 (1H, d, *J* 7.8 Hz, C(3)*H*), 7.17-7.31 (4H, m, C(4)*H* and C(6)*H* and C(9)*H* and C(10)*H*), 7.96-7.98 (1H, dd, *J* 7.5, 1.4 Hz, C(12)*H*), O*H* and N*H* signals not observed; ^{13}C NMR 100.6 MHz, δ_C (MeOD) 31.72 (*C*(15)H$_3$ and *C*(16)H$_3$ and *C*(17)H$_3$), 35.50 (*C*(1)) 113.26 (*C*(13)), 114.76 (*C*(9)H), 117.89 (*C*(6)H), 120.32-120.55 (*C*(3)H and *C*(11)H), 121.62 (*C*(5)H), 130.04 (*C*(4)H), 133.28 (*C*(12)H), 135.05 (*C*(10)H), 141.84 (*C*(7)),

149.58 (*C*(8)), 153.82 (*C*(2)), 171.87 (*C*(14)); HPLC retention time 4.68 min, 2.14 relative to FFA; HRMS: $C_{17}H_{19}NO_2$, Predicted m/z 270.148855, Measured m/z 270.14833 $[M+H]^+$, i-FIT Confidence (%) 100.000000.

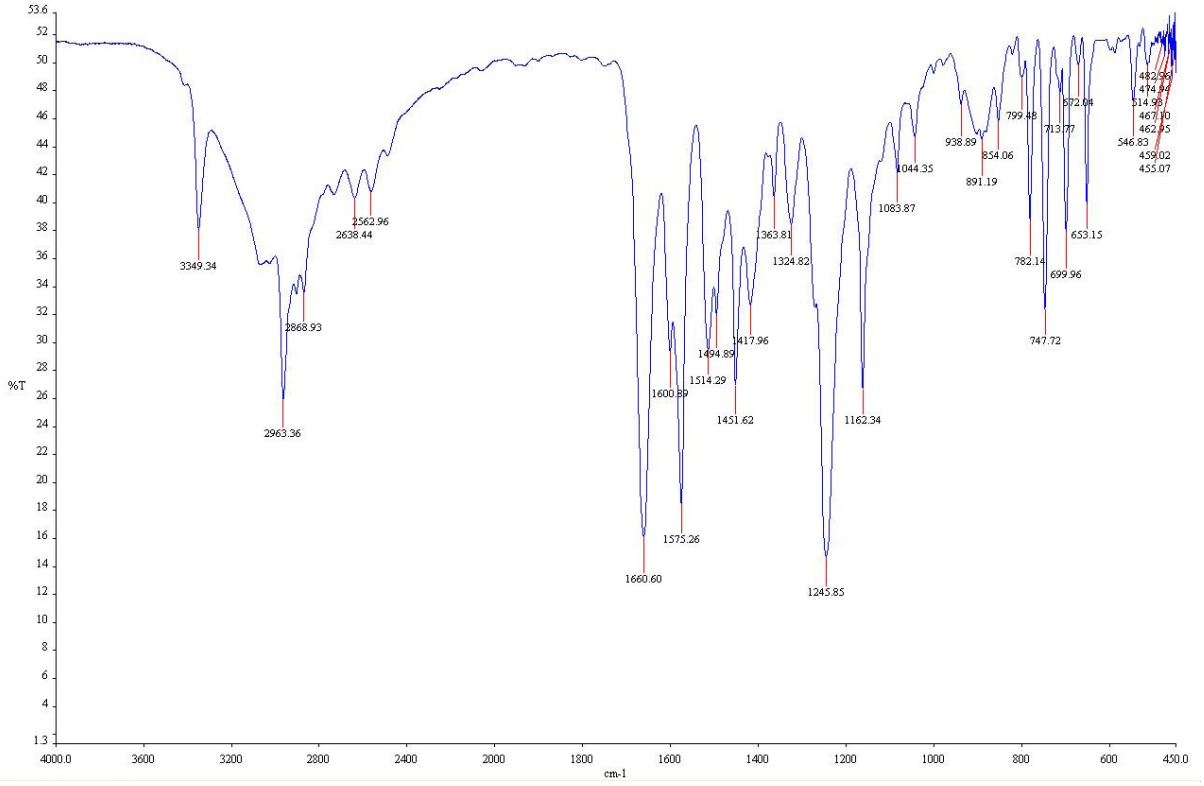

Fig S6. IR spectrum of *t*BuFA.

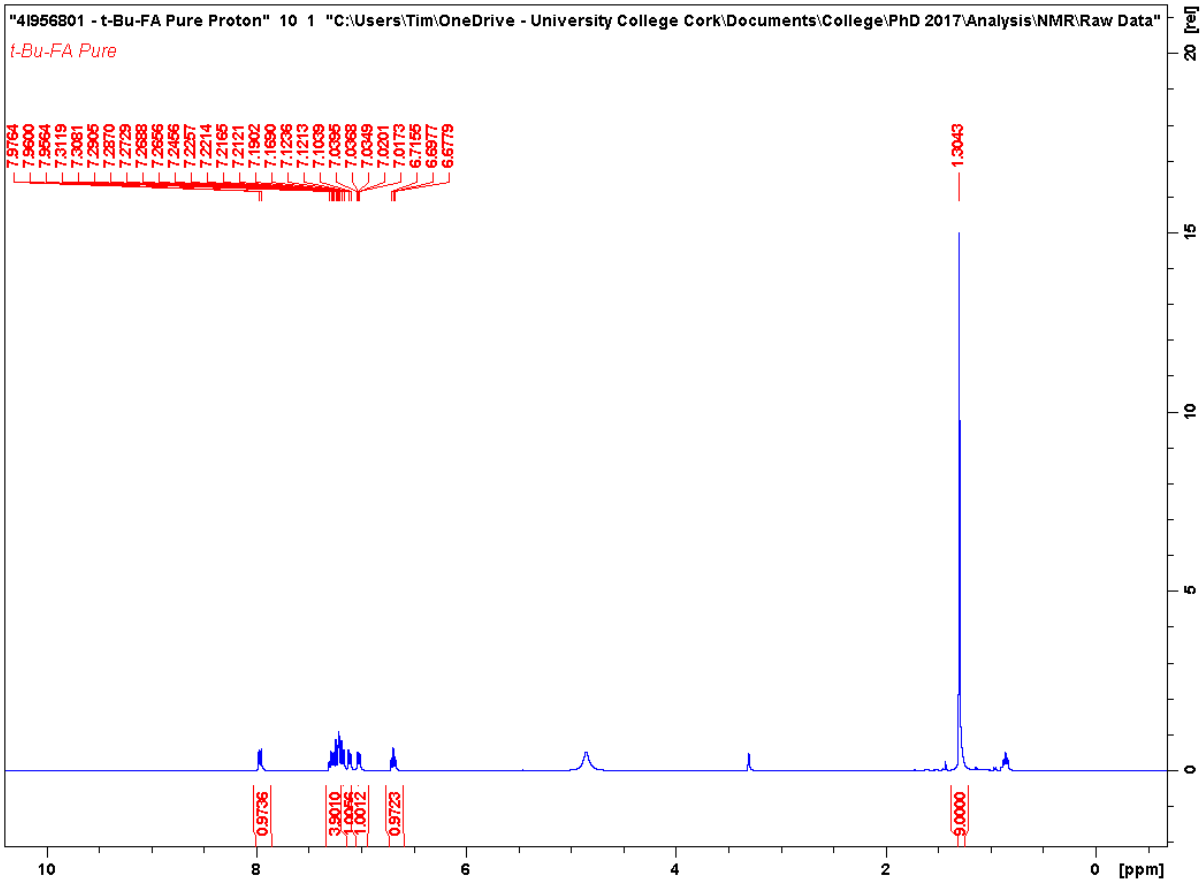

Fig S7. Full ^{1}H NMR spectrum of *t*BuFA showing the position of the 9H *t*-butyl signal outside of the aromatic region.

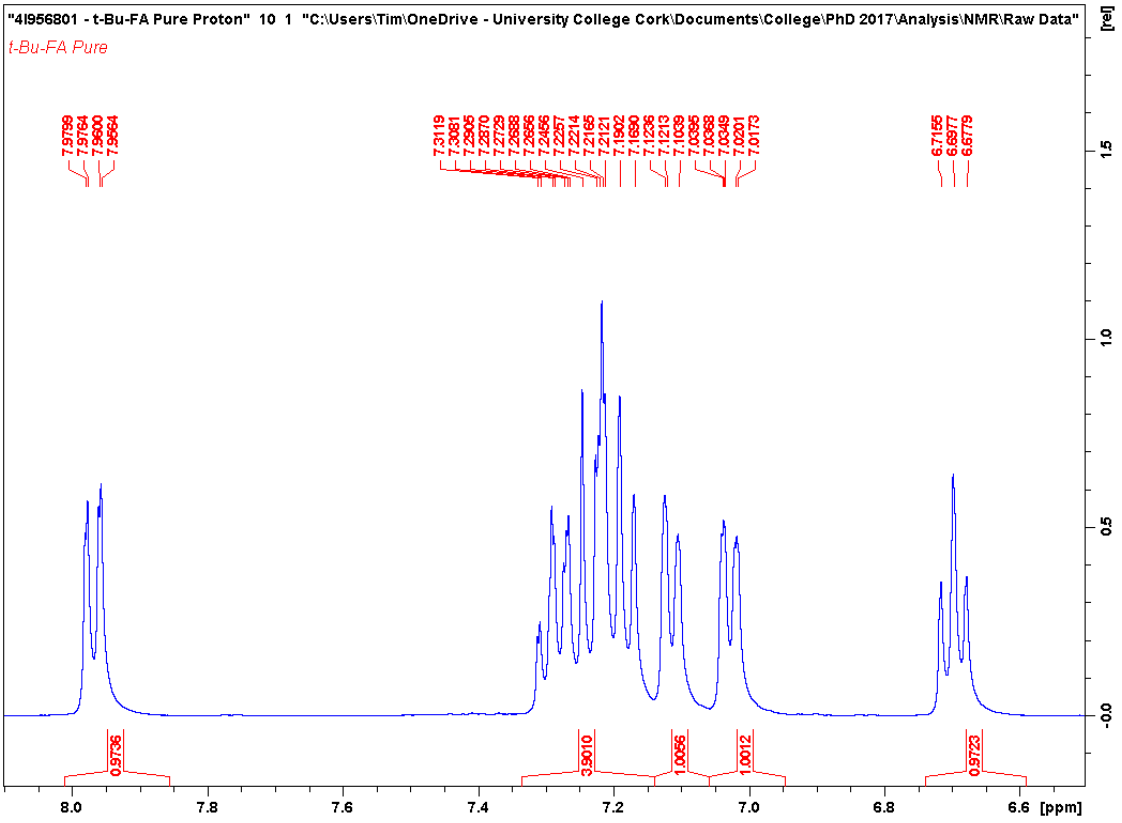

Fig S8. Aromatic region of the ^{1}H NMR spectrum of *t*BuFA.

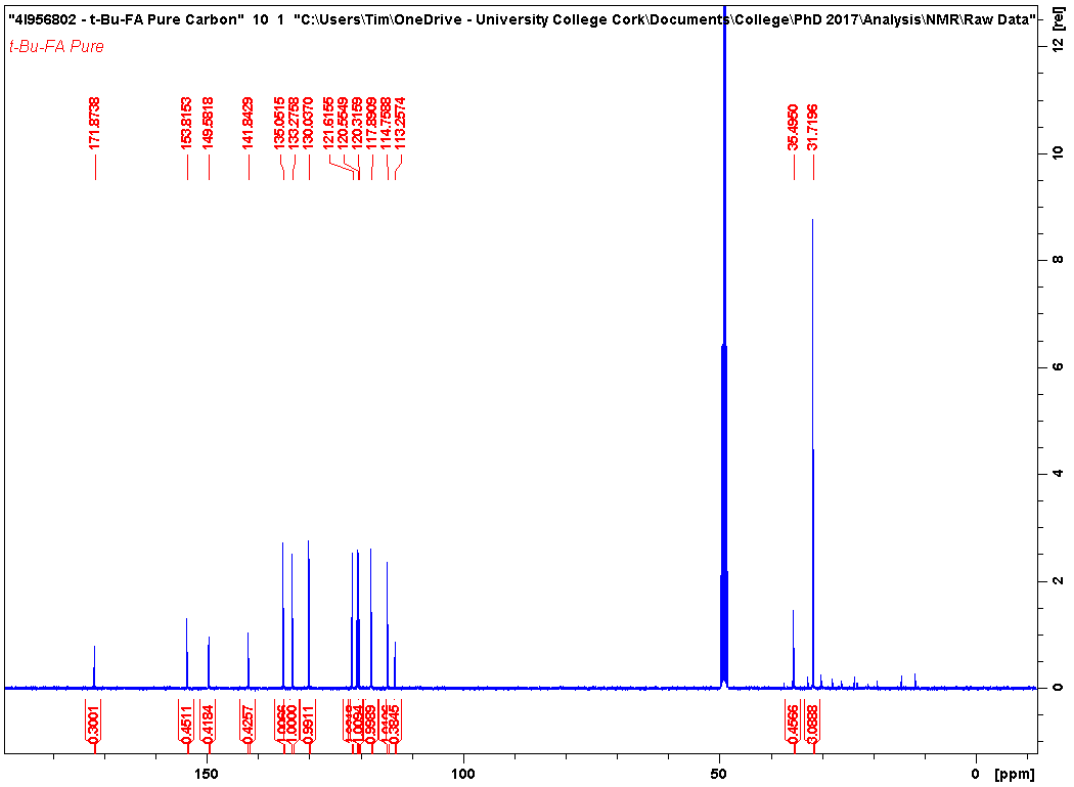

Fig S9. Full ^{13}C NMR spectrum of *t*BuFA showing the position of five quaternary carbon signals as well as the 3C *t*-butyl signal outside the aromatic region.

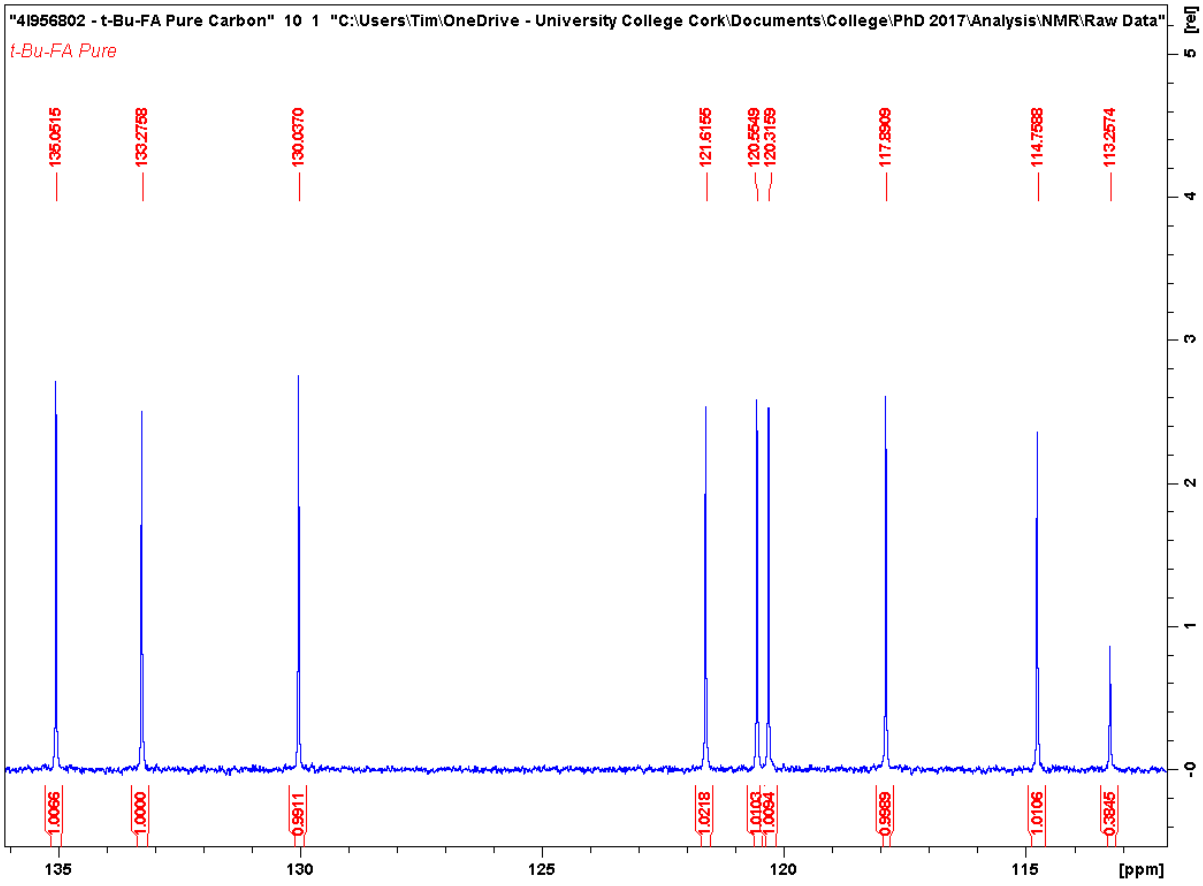

Fig S10. Aromatic region of the ^{13}C NMR spectrum of *t*BuFA.

HPLC Supplemental Information

Calibration Curves

Standard solutions were prepared using MeCN as solvent. The calibration curve for FFA is presented in figure S11. A linear regression curve was fitted to the data points using Excel software (figure S12).

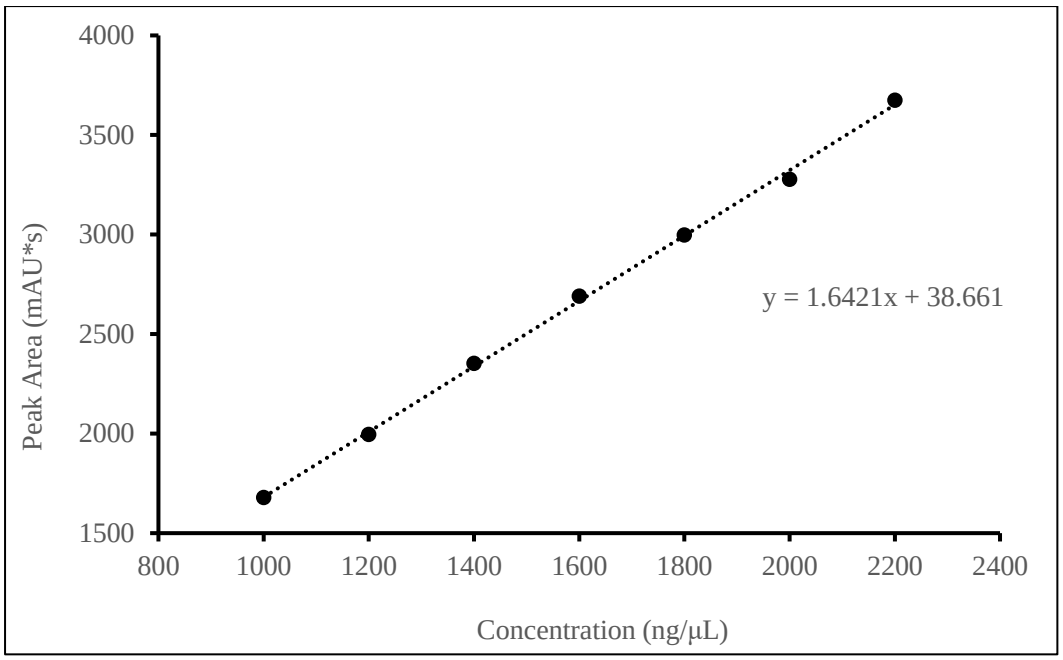

Fig S11. Linear regression curve fitted to the commercial FFA data points, and the equation of that curve.

Residual analysis plots the similarity of the data points to their predicted position as calculated by the regression analysis (figure S12).

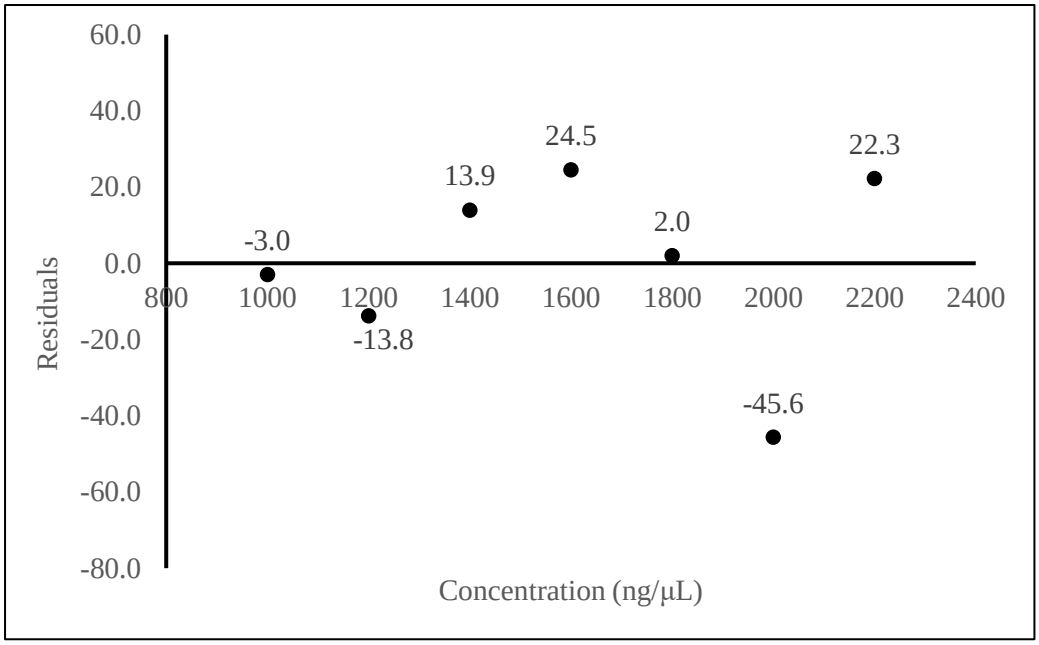

Fig S12. Plot of the regression residuals of the FFA commercial calibration curve.

The regression statistics for the FFA curve are presented below (tables S1 – S3).

Table S1. Regression statistics for the FFA commercial calibration curve, including *r* values.

Multiple R	0.9994083
R Square	0.9988169
Adjusted R Square	0.9985802
Standard Error	26.7487195
Observations	7

Table S2. ANOVA regression statistics for the FFA commercial calibration curve.

ANOVA	df	SS	MS	F	Significance F
Regression	1	3020160.804	3020160.804	4221.085	1.64E-08
Residual	5	3577.470	715.494		
Total	6	3023738.274			

Table S3. Regression coefficient statistics for the FFA commercial calibration curve.

	Coefficients	Standard Error	t Stat	P-value	Lower 95.0%	Upper 95.0%
Intercept	38.661	41.685	0.927	0.396	-68.494	145.81
Concentration (ng μL^{-1})	1.642	0.025	64.970	1.64E-08	1.577	1.707

Examples of HPLC Trace Separation between FFA and the MeFA and tBuFA impurities additive using final method on UHPLC column are given below.

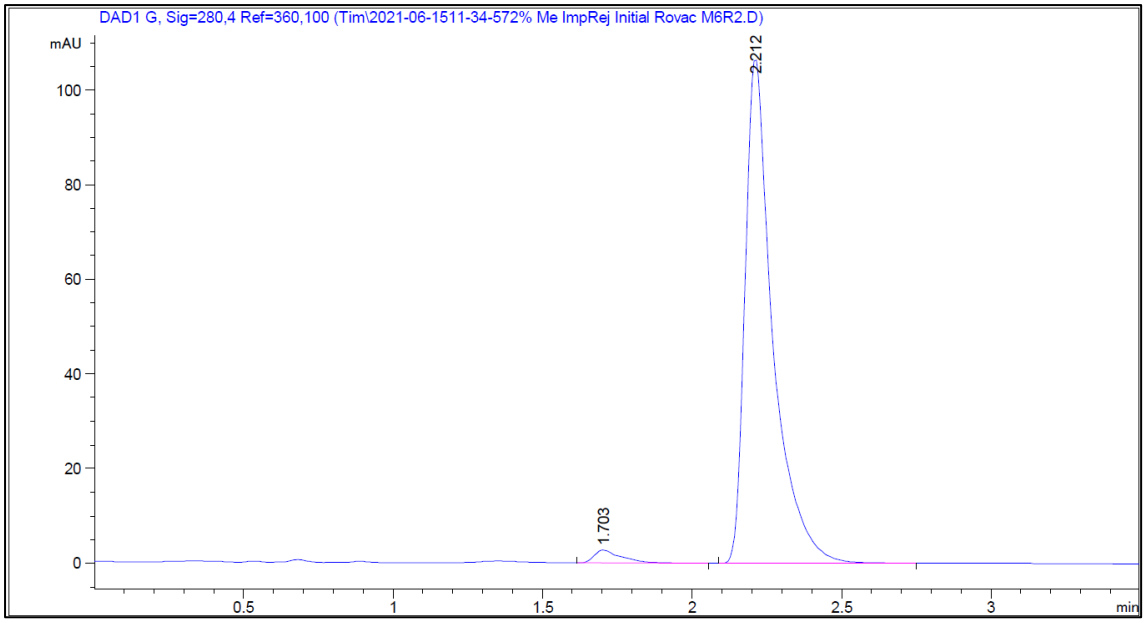

Fig S13. HPLC trace of FFA (right, 2.212 min) containing approx. 2 mol% MeFA (left, 1.703 min).

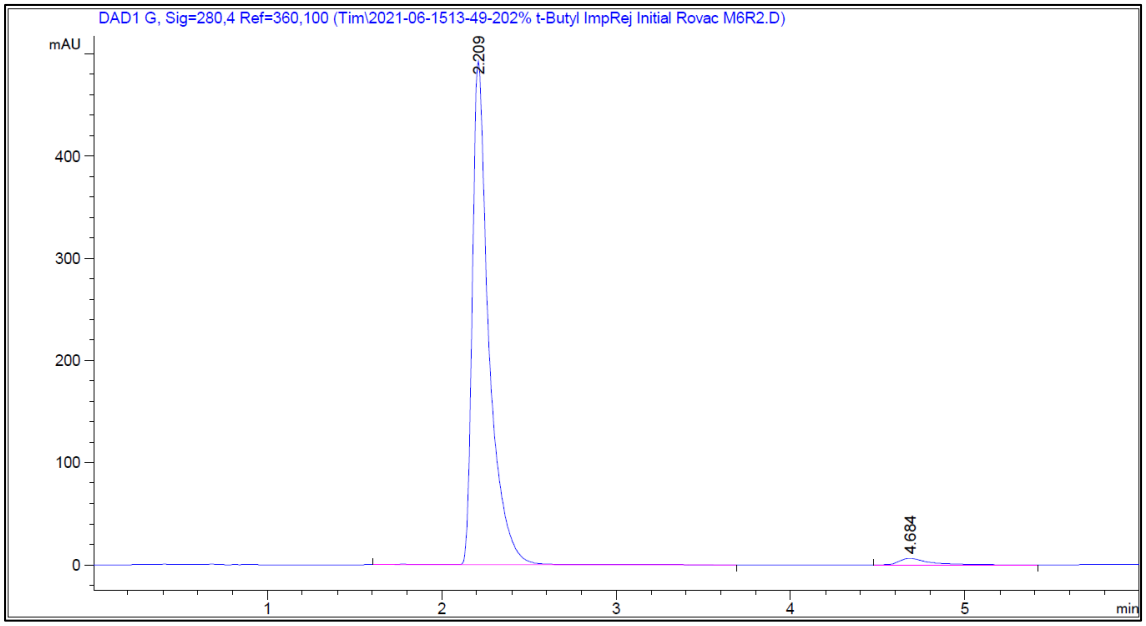

Fig S14. HPLC trace of FFA (left, 2.209 min) containing approx. 2 mol% *t*BuFA (right, 4.684 min)

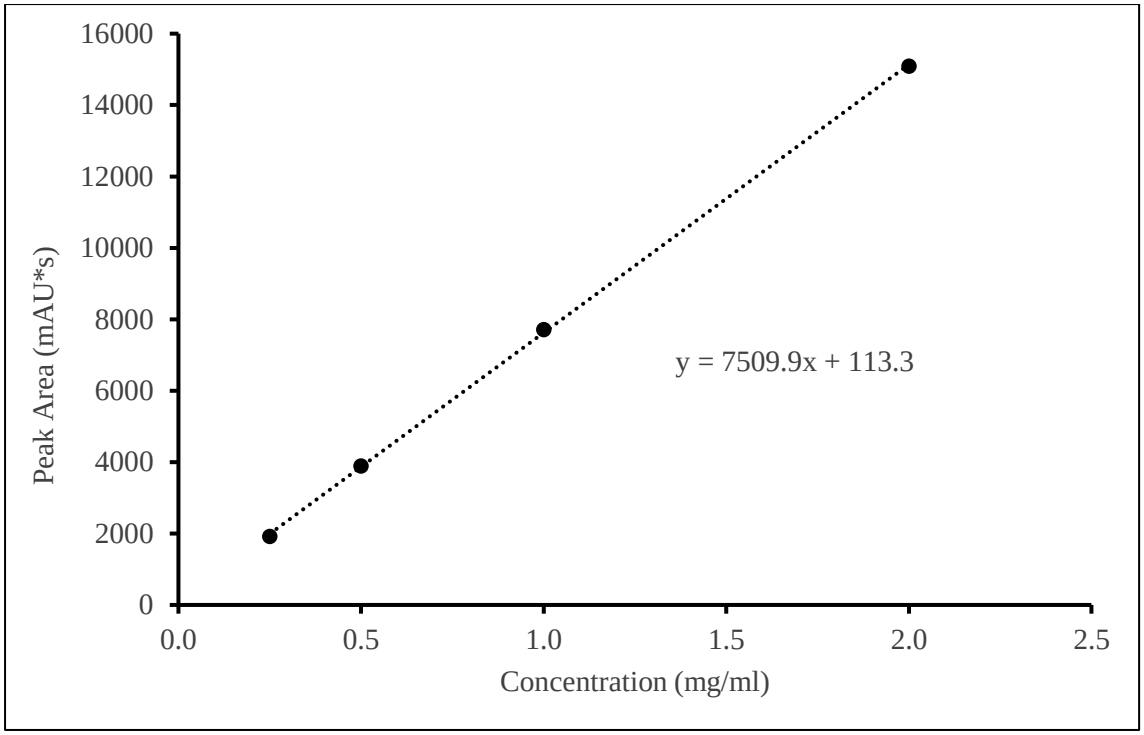

Fig S15. Calibration curve for MeFA with linear regression curve equation.

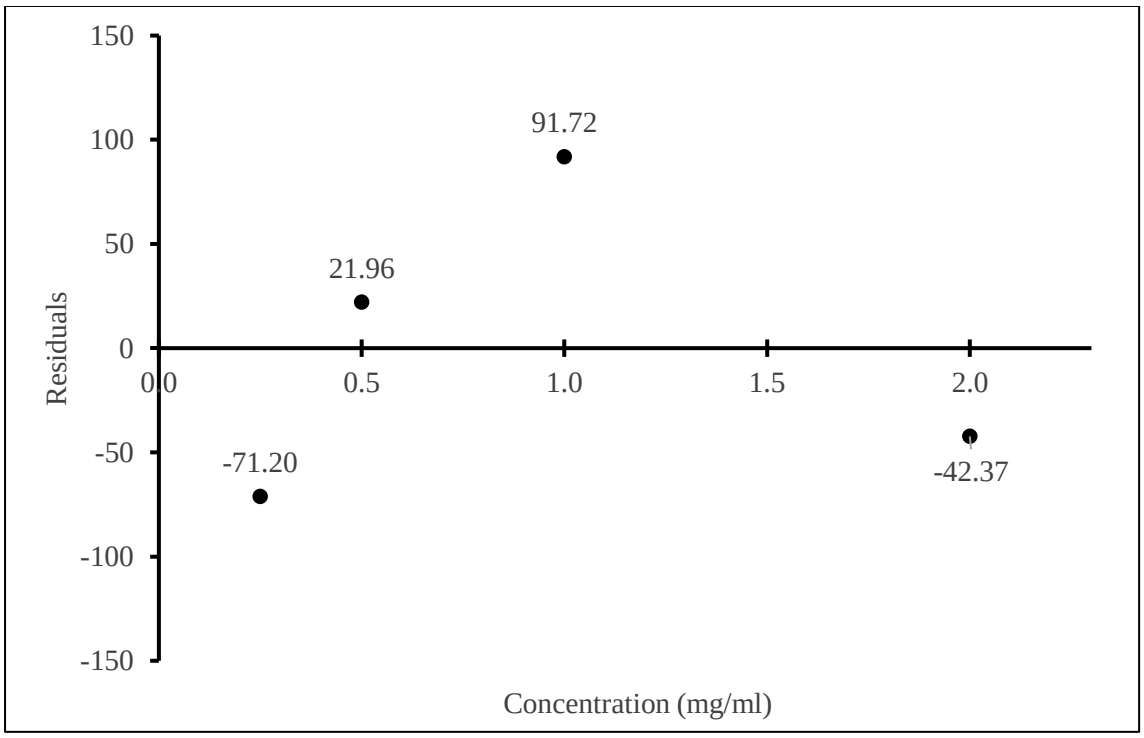

Fig S16. Plot of Residual Values for MeFA Calibration Curve.

Table S4. Residual Statistics for MeFA Calibration Curve.

Multiple R	0.9999223
R Square	0.9998445
Adjusted R Square	0.9997668
Standard Error	88.7653047
Observations	4

Table S5. ANOVA Statistics for MeFA Calibration Curve.

ANOVA	df	SS	MS	F	Significance F
Regression	1	101342056.144	101342056.144	12861.843	7.774E-05
Residual	2	15758.559	7879.279		
Total	3	101357814.703			

Table S6. Residual Coefficients Statistics for MeFA Calibration Curve.

	Coefficients	Standard Error	t Stat	P-value	Lower 95.0%	Upper 95.0%
Intercept	113.302	76.314	1.485	0.276	-215.050	441.654
Concentration (mg/mL)	7509.931	66.219	113.410	7.774E-05	7225.012	7794.849

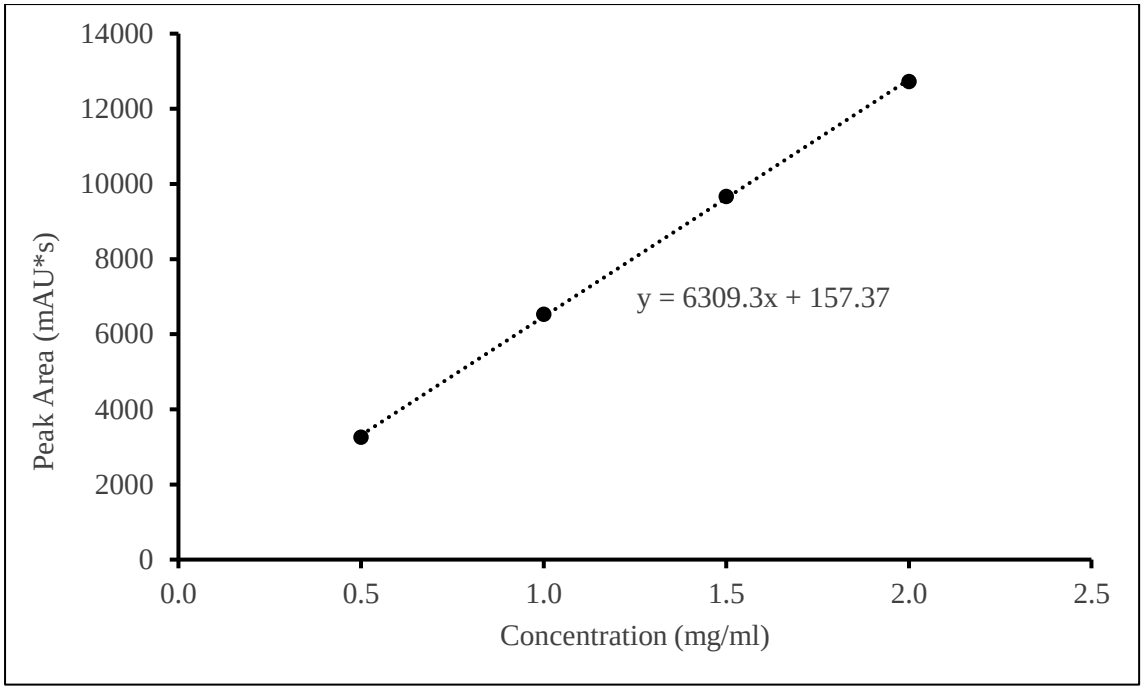

Fig S17. Calibration Curve for *t*BuFA with linear regression curve equation.

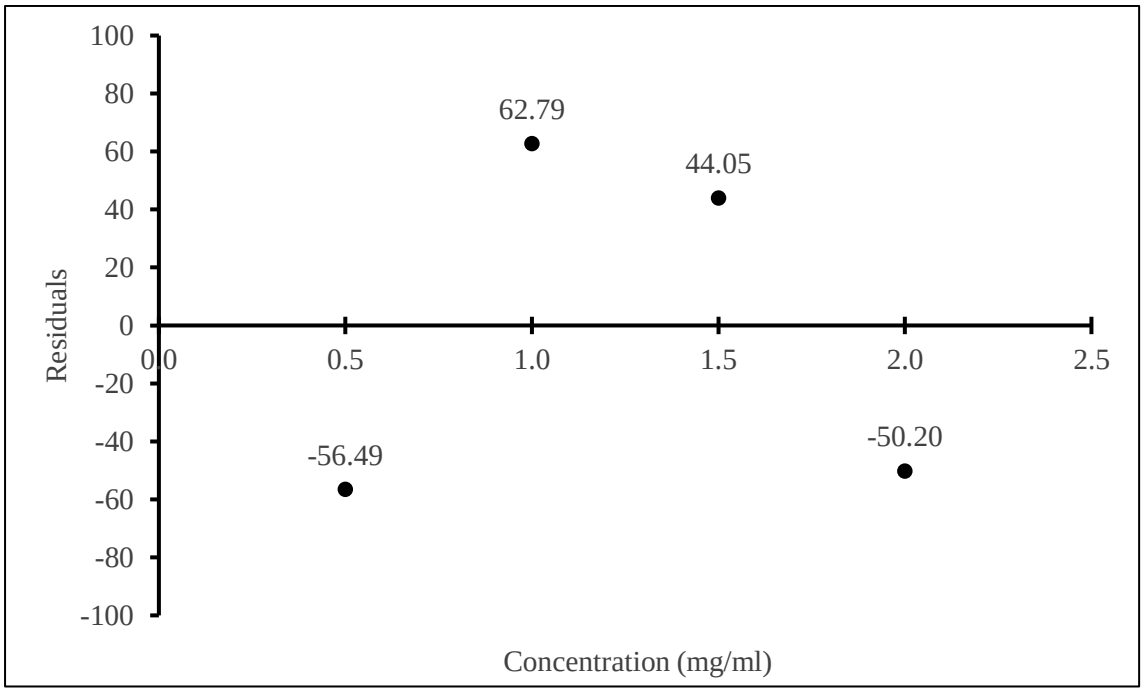

Fig S18. Plot of Residual Values for *t*BuFA Calibration Curve.

Table S7. Residual Statistics for *t*BuFA Calibration Curve.

Multiple R	0.9998835
R Square	0.9997670
Adjusted R Square	0.9996505
Standard Error	76.1415330
Observations	4

Table S8. ANOVA Statistics for *t*BuFA Calibration Curve.

ANOVA	df	SS	MS	F	Significance F
Regression	1	49759483.796	49759483.796	8582.87	1.165E-04
Residual	2	11595.066	5797.533		
Total	3	49771078.862			

Table S9. Residual Coefficients Statistics for *t*BuFA Calibration Curve.

	Coefficients	Standard Error	t Stat	P-value	Lower 95.0%	Upper 95.0%
Intercept	157.374	93.254	1.688	0.234	-243.866	558.613
Concentration (mg/mL)	6309.325	68.103	92.644	1.165E-04	6016.302	6602.349

FFA Polymorphism

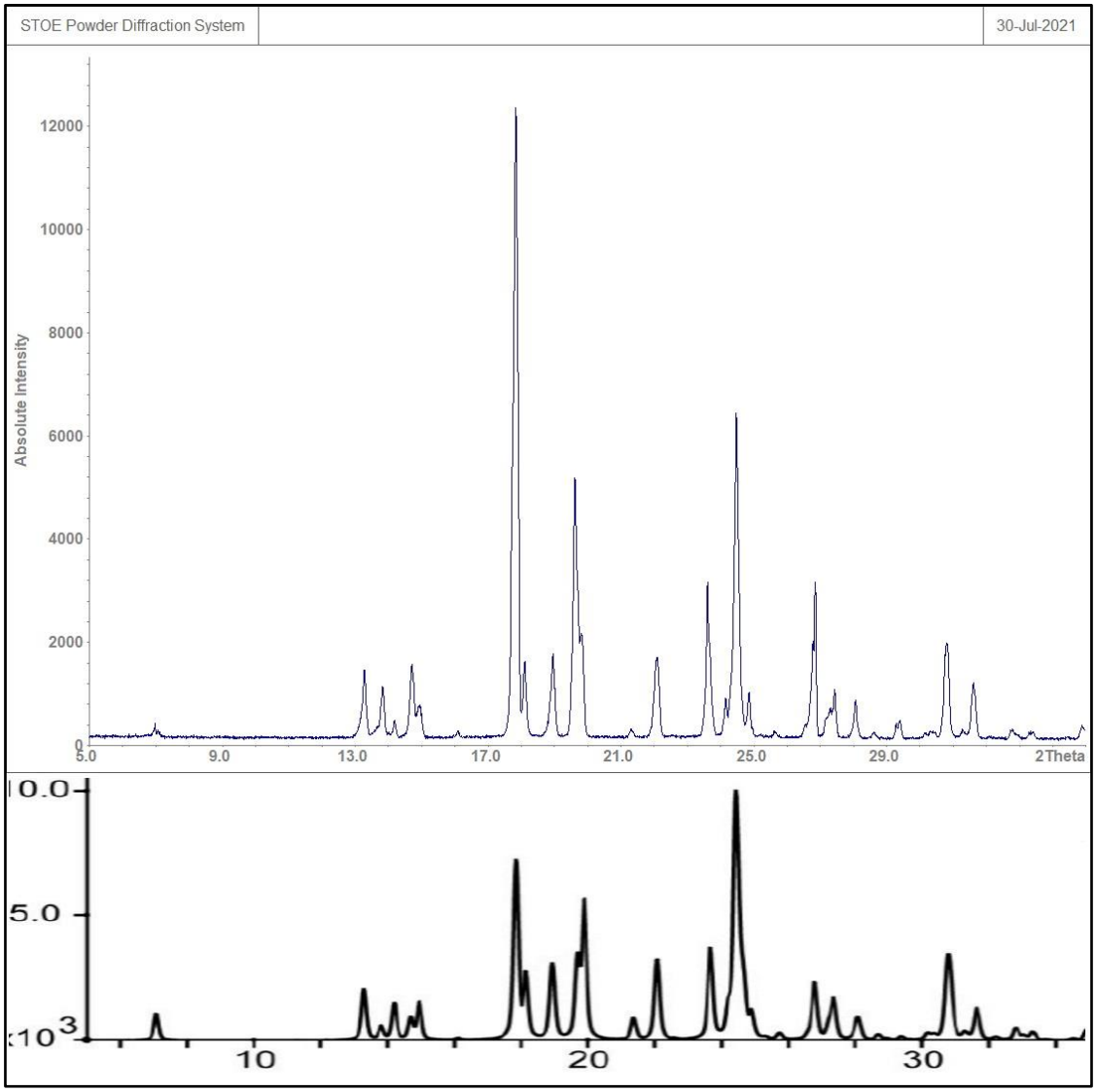

Figure S19. Measured PXRD pattern of commercial FFA (top) *vs.* literature pattern[S3] for Form I FFA (bottom).

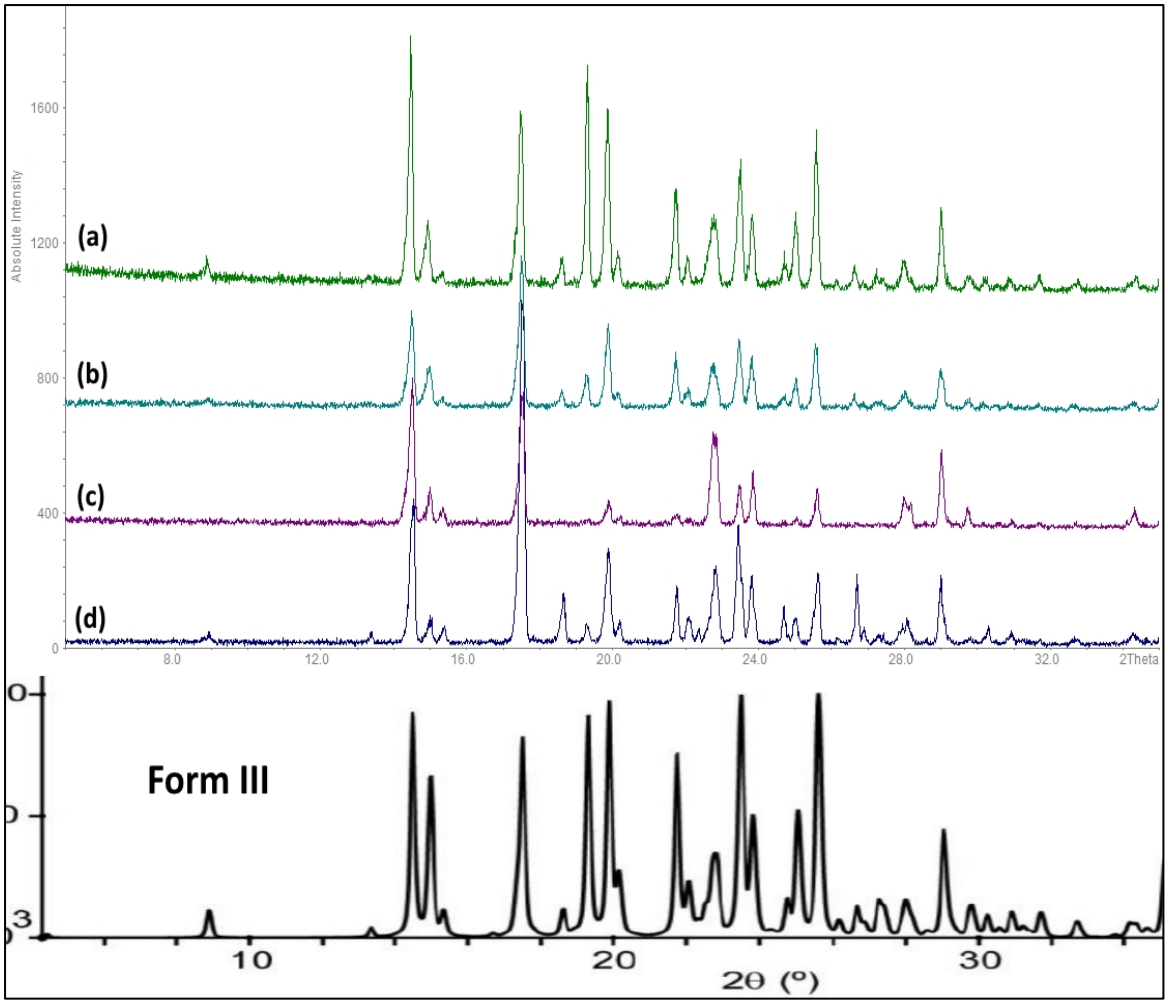

Figure S20. Measured PXRD patterns of FFA recrystallised *via* (a) slow evaporation from MeOH, (b) crystallisation from dichloromethane/hexane mixture with selective dichloromethane evaporation using rotary evaporation, (c) slow cooling of a MeCN solution, and (d) vapour diffusion using MeOH as solvent and hexane as precipitant (top) *vs*. literature pattern[S3] for Form III FFA (bottom).

Solubility Determinations

Two solvents, MeCN and EtOH, were selected for temperature-based solubility studies. The solubility of FFA in these solvents was measured at 10 °C intervals from 40 °C to 70 °C. The saturation points were determined by the excess solid method. The sample flask was immersed in a DrySyn® heating block on an IKA RCT Basic® hot plate, which was controlled at the desired temperature *via* a feedback temperature probe. The suspended solid was agitated in the solvent using a stirrer bar for 1 to 3 hours to ensure complete equilibration and saturation of the solution. After equilibration, 1 mL of saturated solution was removed from the flask through a 0.20 µm membrane syringe filter (Agilent 13 mm, PTFE Econofltr) to ensure the exclusion of undissolved particulates. The solvent was fully evaporated and dried further under high vacuum for at least 2 hours. The residue was redissolved in 100 mL of MeCN and analysed by HPLC (in triplicate). The solubility data is shown in Figure S21.

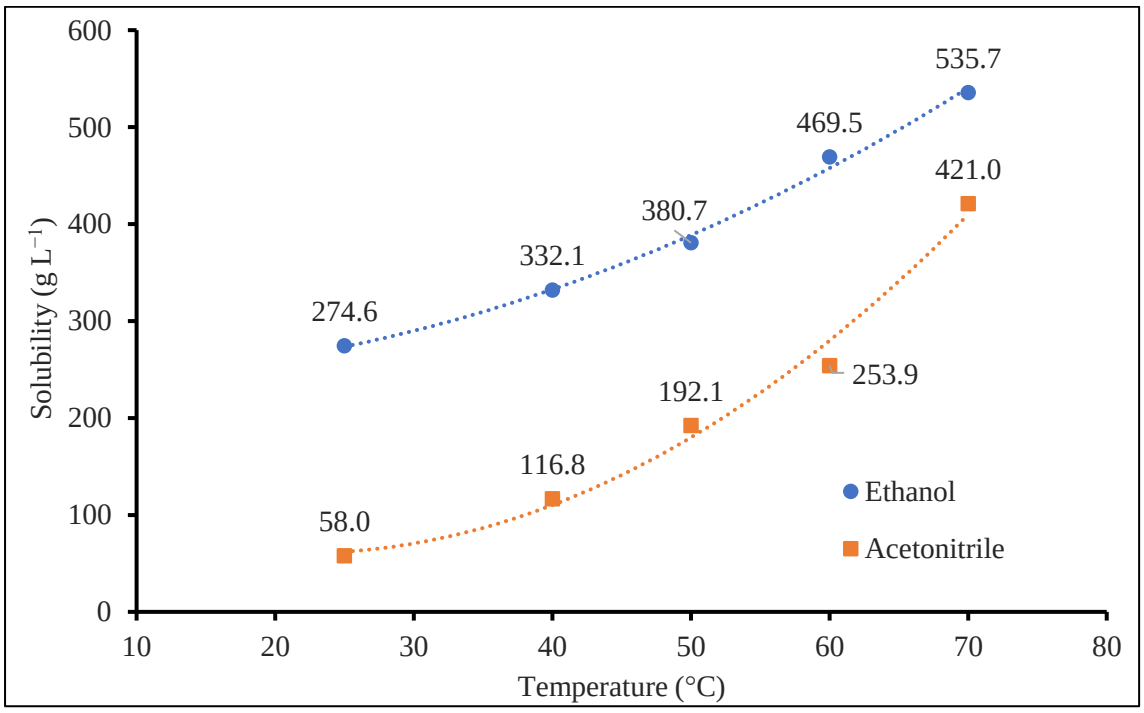

Fig S21. Solubility measurement curves of Form III FFA in EtOH and MeCN at increasing temperatures, from 25 - 70 °C.

Morphology Images

Fig S22. FFA crystals containing approx. 0.5 % MeFA.

Fig S23. FFA crystals containing approx. 5 % MeFA.

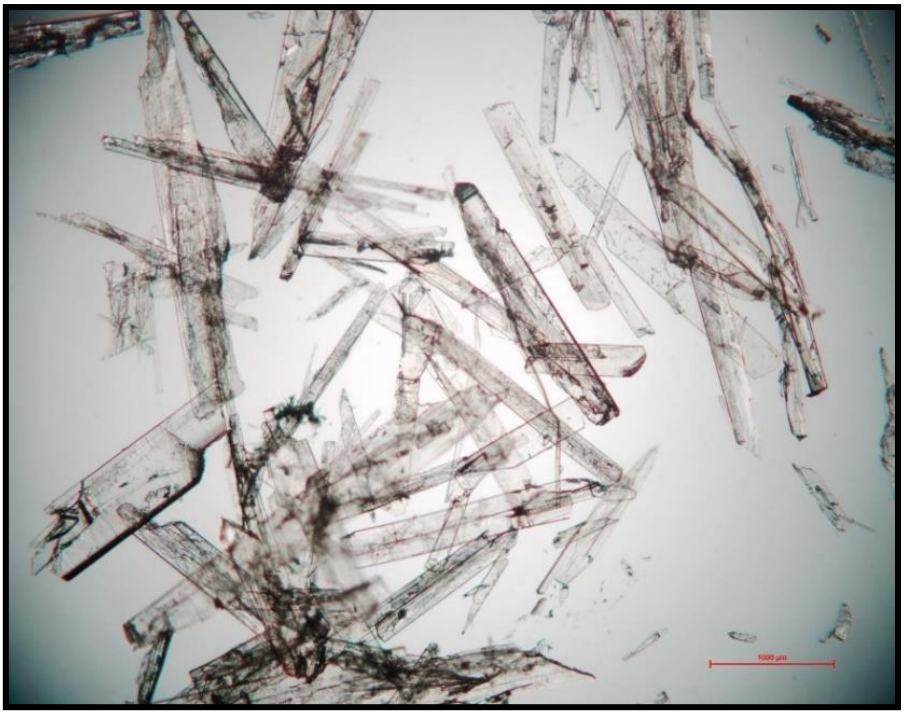

Fig S24. Microscope image (x40) of FFA crystals grown with 0.5% MeFA impurity.

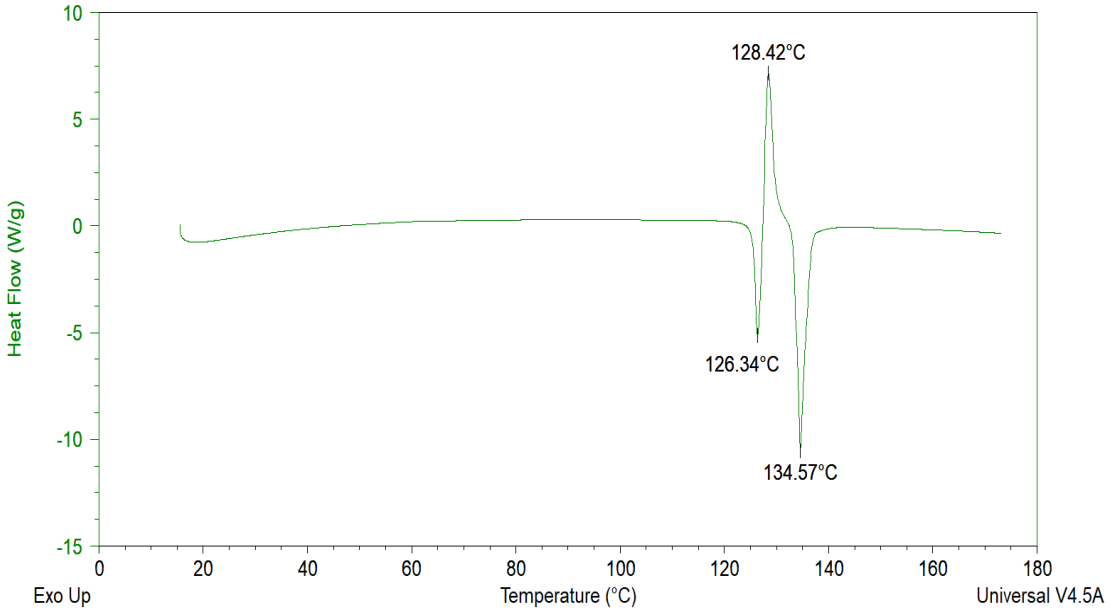

Fig. S25. DSC curve of Form III FFA heated at a rate of 20 °C min^{-1}, exhibiting melting of Form III, recrystallisation of Form I and melting of Form I.

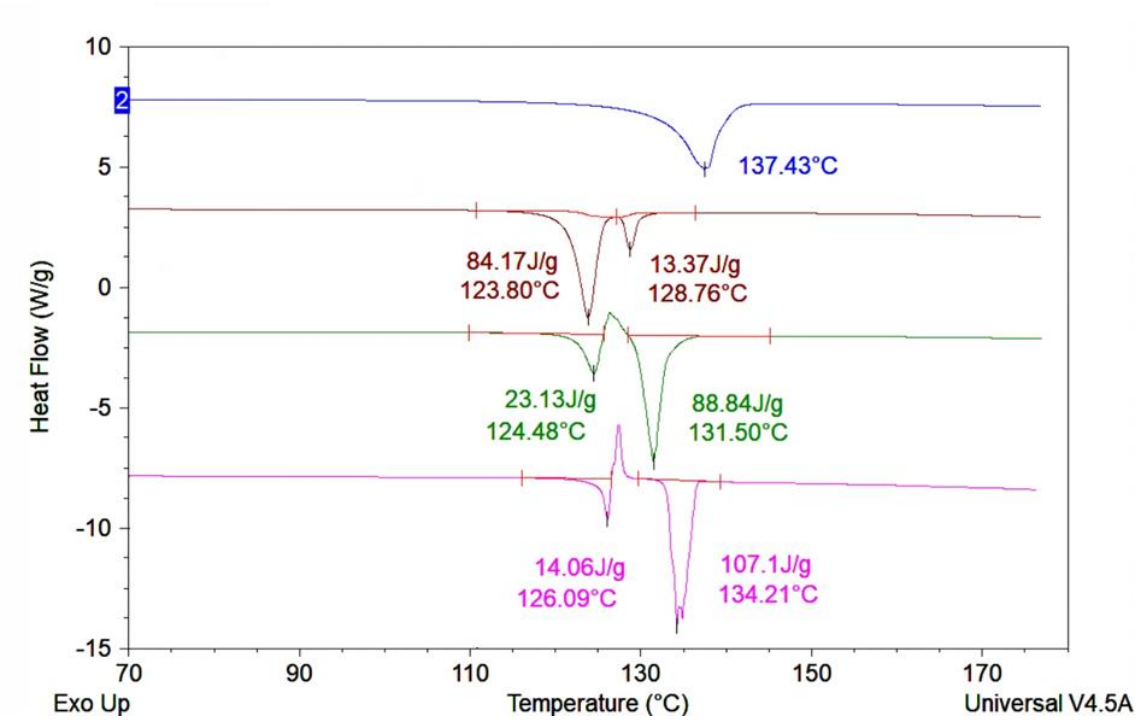

Fig S26. Top to bottom, DSC curves of pure MeFA, FFA containing 20 % MeFA, FFA containing 10 % MeFA, and pure Form III FFA, labelled with peak area and peak max values; obtained at heating rates of 10 °C min^{-1}.

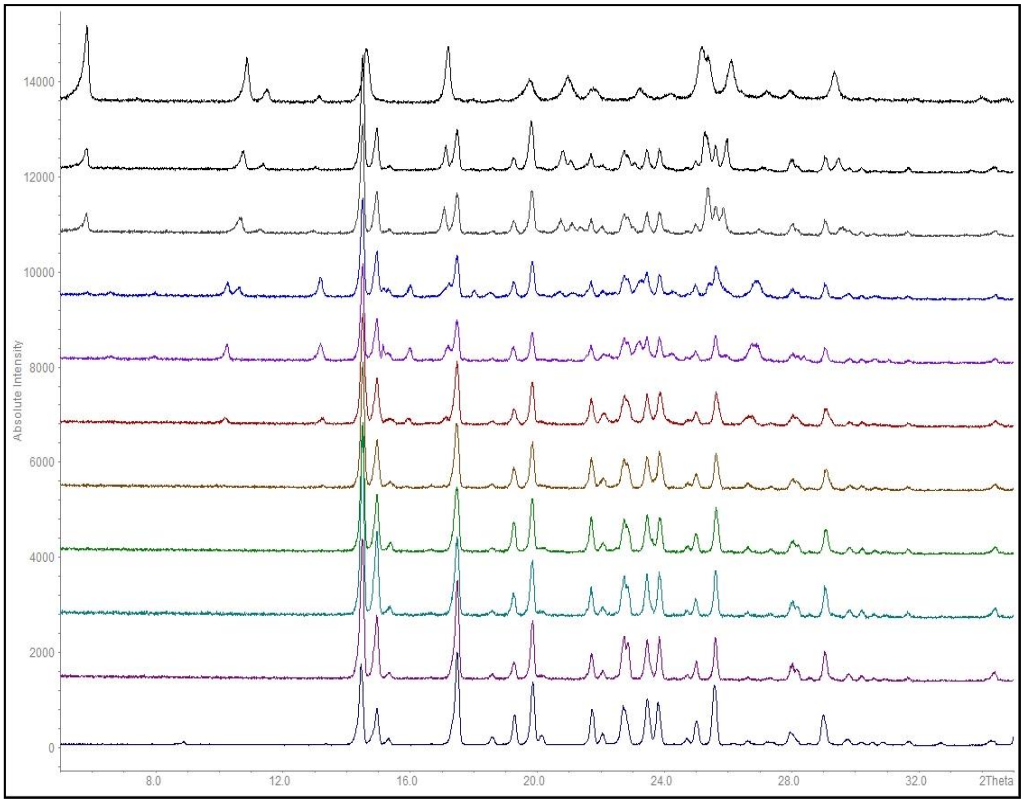

Fig. S27. Bottom to top: PXRD patterns of pure FFA Form III compared to FFA containing increasing levels of MeFA (approx. 10, 20, 30, 40, 50, 60, 70, 80, and 90 %) and pure MeFA.

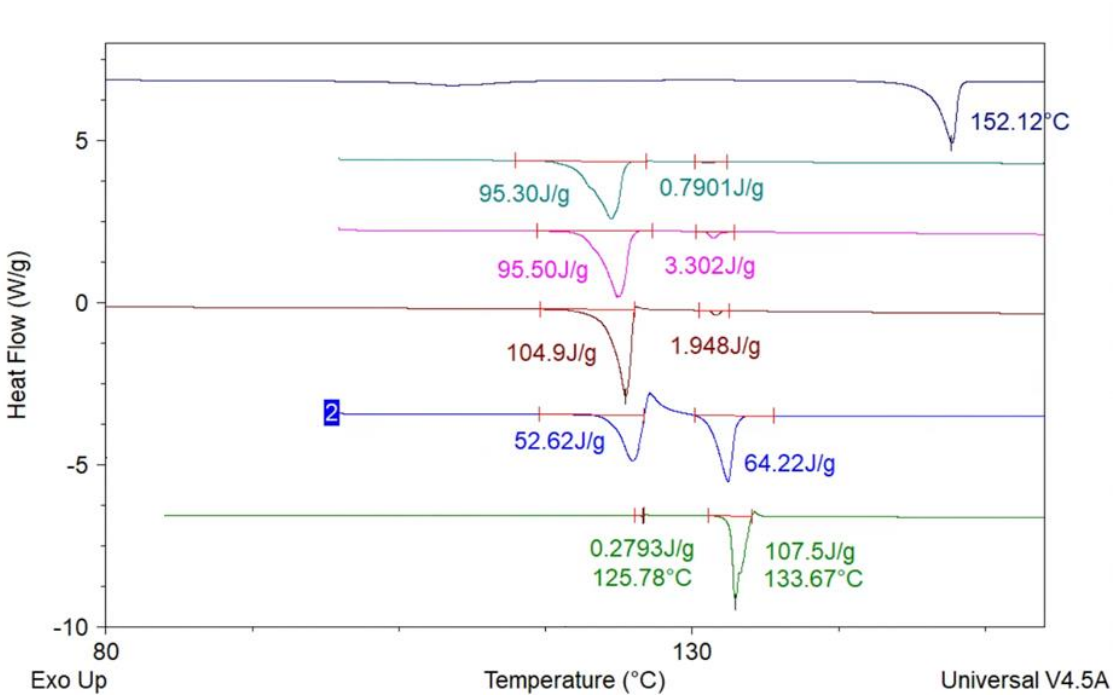

Fig S28. Bottom to top: DSC curves of pure Form III FFA and FFA containing 2, 3, 4, and 5 % *t*BuFA, and pure *t*BuFA, collected at heating rates of 2 - 3 °C min^{-1}, labelled with peak area and peak max values.

Fig S29. Microscope images (x40) of FFA crystals (containing ca. 5% MeFA) after four partial dissolution stages, PD1 to PD4.

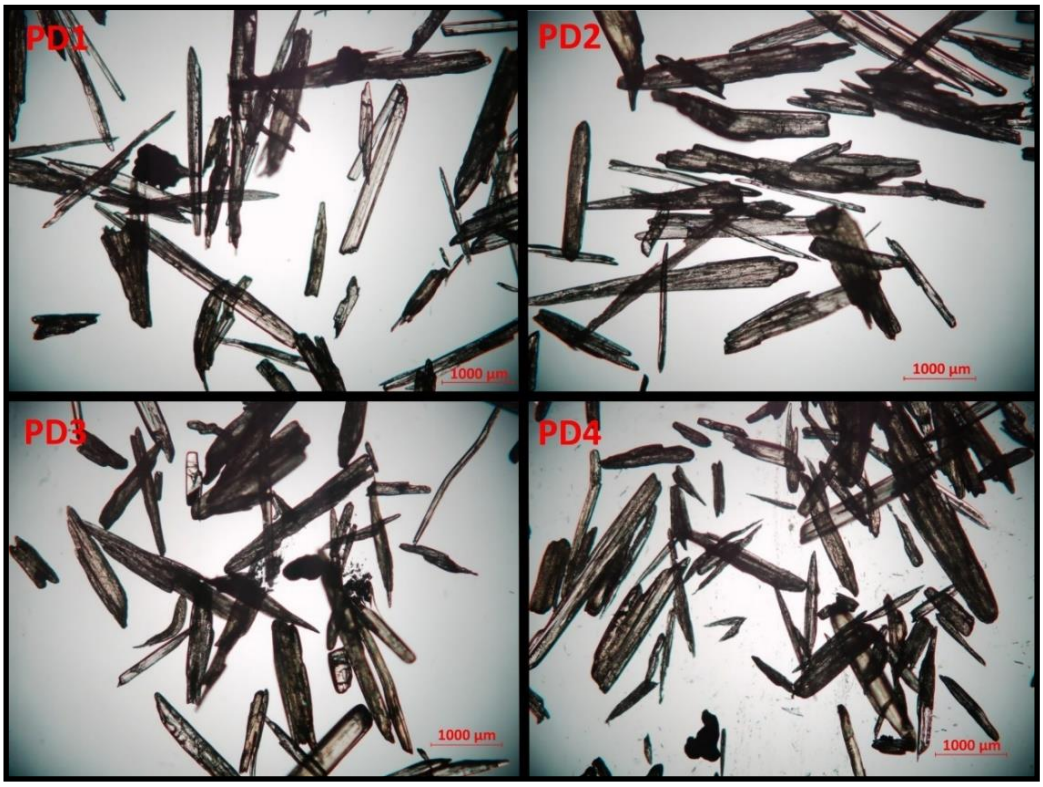

Fig S30. Microscope images (x40) of FFA crystals (containing ca. 2% *t*BuFA) after four partial dissolution stages, PD1 to PD4.

References

S1. Kaltenbronn, J. S.; Scherrer, R. A.; Short, F. W.; Jones, E. M.; Beatty, H. R.; Saka, M. M.; Winder, C. V.; Wax, J.; Williamson, W. R. N. ChemInform Abstract: STRUCTURE-ACTIVITY RELATIONSHIPS IN A SERIES OF ANTIINFLAMMATORY N-ARYLANTHRANILIC ACIDS. *Chem. Information Sd.* **1983**, *14* (37), 621–627.

S2. Sowinski, F.; Yale, H. L., *J. Med. Pharm. Chem.* **1962**, *5* (1), 54–63.

S3. López-Mejías, V.; Kampf, J. W.; Matzger, A. J. *J. Am. Chem. Soc.* **2012**, *134* (24), 9872–9875.